

# Magneto-optical properties of Co/Pd superlattice thin films

Sung-Chul Shin and Anthony C. Palumbo

Diversified Technologies Group Research Laboratories, Eastman Kodak Company,  
Rochester, New York 14650

(Received 13 February 1989; accepted for publication 11 September 1989)

We present the remnant polar Kerr rotation and ellipticity for a Co/Pd superlattice. The magneto-optical properties of Co/Pd superlattice thin films have been investigated by measuring both the polar Kerr and ellipticity hysteresis loops at a wavelength of 780 nm. It was found that the remnant Kerr rotation was strongly dependent on the thickness of Co and Pd sublayers as well as the total film thickness. In this system, the maximum polar Kerr rotation of  $0.43^\circ$  was observed at the film thickness of 110 Å, where each bilayer was composed of 2-Å-thick Co and 9-Å-thick Pd sublayers.

## I. INTRODUCTION

Materials exhibiting the polar Kerr effect are of interest for the application to magneto-optical recording which enables erasable high-density data storage.<sup>1,2</sup> In magneto-optical recording, thermomagnetically written data on a magneto-optical recording medium can be read by irradiating the medium with a linearly polarized laser beam and detecting the change of the incident laser beam polarization caused by the interaction of the light with the magnetization. The amount of this change in polarization in the reflection is called the polar Kerr rotation. Currently, amorphous thin alloy films consisting of primarily rare earth and transition metals are the most popular materials for magneto-optical recording. An inherent disadvantage of these materials is that they are highly subject to corrosion and must be protected.<sup>3</sup> One solution would be to consider a multilayer stack of elements or alloys which are not so susceptible to corrosion.

Perpendicular magnetic anisotropy of a material is necessary to develop the polar Kerr effect. Neel<sup>4</sup> first pointed out that the magnetic surface anisotropy which favors perpendicular magnetic anisotropy might develop at the surface of a ferromagnetic material. Quite recently, Draaisma and De Jonge<sup>5</sup> reported that multilayered Co/Pd films had perpendicular magnetic anisotropy. However, little has been investigated on the magneto-optical properties of this system. In this paper, we present magneto-optical properties of Co/Pd superlattice thin films.

## II. EXPERIMENT

Co/Pd superlattice thin films were prepared by *e*-beam evaporation of Co and Pd on quartz substrates in a vacuum system maintained at about  $2 \times 10^{-6}$  Torr during the deposition. The superlattice structure was achieved by alternately exposing the substrate to two *e*-beam sources via a rotating substrate mount. Two *e*-beam sources were physically separated by stainless shields to prevent cross contamination of their evaporated fluxes. The sublayer thickness of each constituent in one repeat distance was varied by changing the deposition rate of each constituent, which was monitored by a corresponding quartz crystal sensor. Typical deposition rates of Co and Pd were 0.9–2.8 Å/s and 2–10 Å/s, respec-

tively. The samples will be designated by *t*-Co/*t*-Pd, where *t*-Co and *t*-Pd are the thicknesses of Co and Pd in one repeat distance, respectively.

The polar Kerr rotation ( $\theta_k$ ) and ellipticity ( $\epsilon$ ) hysteresis loops were simultaneously measured at 780 nm with a photoelastic modulator (PEM) based instrument.<sup>6</sup> *S* polarized laser light pulsed at 3 kHz passed through the bore of a magnet striking the sample at an incident angle of  $1^\circ$  and returned through the bore. Then, it was deflected via a prism through the PEM (the optic axis is perpendicular to the plane of incidence of the light on the sample) and analyzer and was focused onto a photodetector.

Simultaneous measurement of  $\theta_k$  and  $\epsilon$  signals required two trade-offs. First, the phase modulation amplitude of the PEM was set at  $0.76547\pi$  to simplify the following mathematical relationships<sup>7</sup>:  $\theta_k \propto S(2f)/S_{dc}$  and  $\epsilon \propto -S(f)/S_{dc}$ , where  $f = 50$  kHz is the frequency of the PEM,  $S(2f)$  is the signal at  $2f$  on the detector, and  $S_{dc}$  is the dc light level on the detector. For  $\theta_k$  and  $\epsilon$  less than  $3^\circ$ , the error for using mathematical approximations is less than 0.5% for  $\epsilon$  and 1.0% for  $\theta_k$ . Second, the analyzer was set to  $45^\circ$  (to the plane of incidence of the light on the sample), because it optimized Kerr and ellipticity signals.<sup>6</sup>

$S_{dc}$ ,  $S(f)$ , and  $S(2f)$  were measured by connecting three lock-in amplifiers to the output of the detector. The frequency generator from one lock-in was used to control the pulse frequency of the laser driver and measured a voltage proportional to  $S_{dc}$ . The second lock-in measured a voltage proportional to  $S(f)$  by referencing the PEM fundamental frequency. The third lock-in measured a voltage proportional to  $S(2f)$  by referencing twice the PEM fundamental frequency. With a sample in place, the Kerr rotation and ellipticity were calibrated by placing a quarter-wave plate (QWP) in the path of the incident (linearly polarized) beam and making measurements before and after rotating it by  $4^\circ$ . Note, the azimuthal angle and the arctangent of the ellipticity of the elliptically polarized light are equivalent to the angle between the optic axis of the QWP and the polarization of the incident light. A computer was used to ramp the current in the magnet, measure the lock-in voltages and a voltage proportional to the magnetic field, and produce the plots of the hysteresis loops.

### III. RESULTS AND DISCUSSION

Let's examine the difference between alloy and superlattice thin films of Co/Pd. In Figs. 1(a) and 1(b), the Kerr hysteresis loops (inset ellipticity) of a 2-Å-Co/9-Å-Pd superlattice film and a CoPd alloy film having a similar composition are used for the comparison. A dramatic difference between the two films can be clearly seen; the alloy film does not develop any remnant Kerr angle (the Kerr angle at zero applied field), while the superlattice film provides a remnant Kerr angle of 0.17°. We want to emphasize that a suitable magneto-optical recording medium has remnant Kerr rotation since the remnant Kerr rotation (not the saturated one) is used in the readout process. The squareness in the Kerr and ellipticity hysteresis loops of the superlattice film implies perpendicular magnetic anisotropy, whereas the alloy film with small coercivity and a monotonic increasing Kerr rotation implies in-plane anisotropy.

As seen in the inset of Fig. 1(a), a Co/Pd superlattice thin film generally develops the remnant ellipticity. The ellipticity represents a phase difference in the two orthogonal linear polarizations of the reflected beam. Therefore, the maximum Kerr rotation of a medium is obtained by eliminating the ellipticity using an appropriate phase plate in the reflected beam. For small degrees of Kerr rotation and ellipticity, the phase difference  $\delta$  between two polarizing directions can be calculated by<sup>8</sup>

$$\delta \approx \tan^{-1}(\epsilon/\theta_K), \quad (1)$$

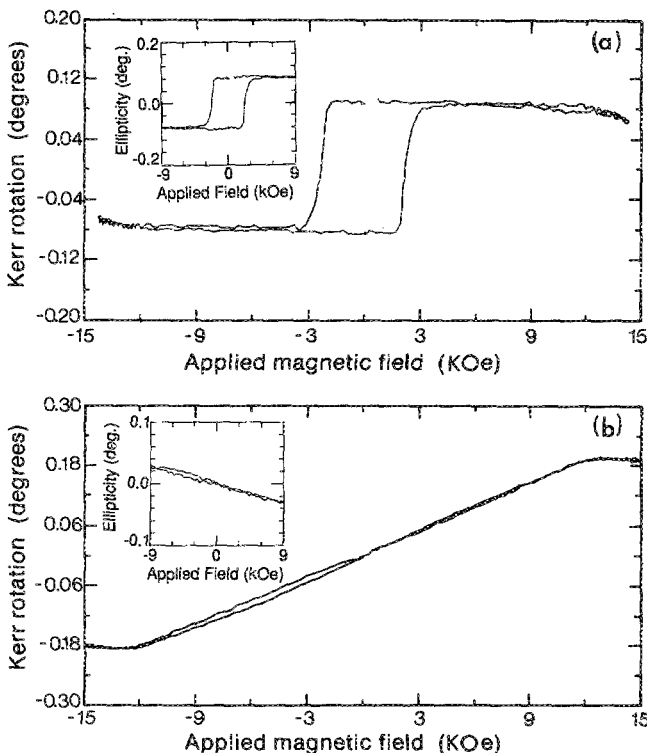


FIG. 1. (a) The polar Kerr rotation hysteresis loop of a 2-Å-Co/9-Å-Pd superlattice film and (b) the polar Kerr hysteresis loop of a CoPd alloy film having a similar composition. The inset in each figure shows the  $-1\times$  ellipticity loop.

where  $\epsilon$  and  $\theta_K$  are the ellipticity and the Kerr rotation measured without a phase plate, respectively. Then, the maximum Kerr rotation, obtainable at the zero ellipticity, is given by

$$\theta_K^{\max} \approx (\theta_K^2 + \epsilon^2)^{1/2}. \quad (2)$$

For example, the Kerr rotation angle of the sample in Fig. 1(a) was maximized up to 0.23° by eliminating the phase difference  $\delta = 42^\circ$ .

The importance of measuring the ellipticity became apparent for a 2-Å-Co/15.6-Å-Pd superlattice film exhibiting ellipticity but no Kerr rotation as shown in Figs. 2(a) and 2(b). Even though the sample does not develop any Kerr rotation, we can conclude that it has perpendicular anisotropy because it has a square ellipticity loop. Using Eq. (1), the phase difference  $\delta$  is calculated as 90°. So, the ellipticity can be converted into only Kerr rotation by introducing a quarter-wave plate in the path of a reflected beam, as demonstrated in Figs. 2(c) and 2(d). Now, all the references to Kerr rotation will refer to the maximum Kerr rotation obtained by using Eq. (2).

Figure 3 shows the dependence of the remnant ( $H = 0$  kOe) and saturated ( $H = 15$  kOe) Kerr rotation angles on the thickness of Pd sublayer. All samples had the same thickness of a 2-Å-Co sublayer within a 10% variation. By increasing the repeat distance, the number of bilayers was reduced to obtain films with similar total thicknesses in the range of about 1300 Å. The Kerr rotation angle in the figure is the maximum value obtained at the zero ellipticity as described earlier. In Fig. 3, it is interesting to note that the remnant Kerr rotation has a broad maximum in the range of 7–9 Å, and it decreases rapidly for Pd thicknesses thinner than 7 Å. The dependence of the remnant magnetization measured from  $B$ - $H$  hysteresis loops showed a similar thickness dependence. Therefore, the dependence of the magnetization seems to be responsible for the behavior of the remnant Kerr rotation. A rapid decrease of the remnant Kerr rotation for a less than 7-Å-Pd sublayer thickness implies that ferromagnetic interaction between two Co sublayers neighboring a Pd sublayer is enhanced with thinning of the Pd sublayer. Therefore, it approaches the magnetic behavior of a Co thick film exhibiting in-plane magnetic anisotropy. Figure 3 shows that the saturation Kerr rotation is monotonically decreased with increasing the thickness of the Pd sublayer. This is expected because the saturation magnetization is proportional to the Co concentration.

The Kerr rotation was very sensitive to the Co sublayer thickness. As shown in the inset of Fig. 3, we observed a fourfold drop in the remnant Kerr rotation as the sublayer thickness goes from one monolayer (2 Å) to two monolayers. This is consistent with a fivefold drop seen in the remnant magnetization.<sup>5</sup>

In Fig. 4, we show the dependence of the Kerr rotation  $2\theta_K$ , reflectivity  $R$ , and figure-of-merit  $R\theta_K^2$  on the total film thickness. Each bilayer was composed of a 2-Å-Co/9-Å-Pd, and the total number of bilayers was varied from 3 to 114 which corresponded to a total film thickness of from 33 to 1318 Å. A variation of the bilayer thickness among samples

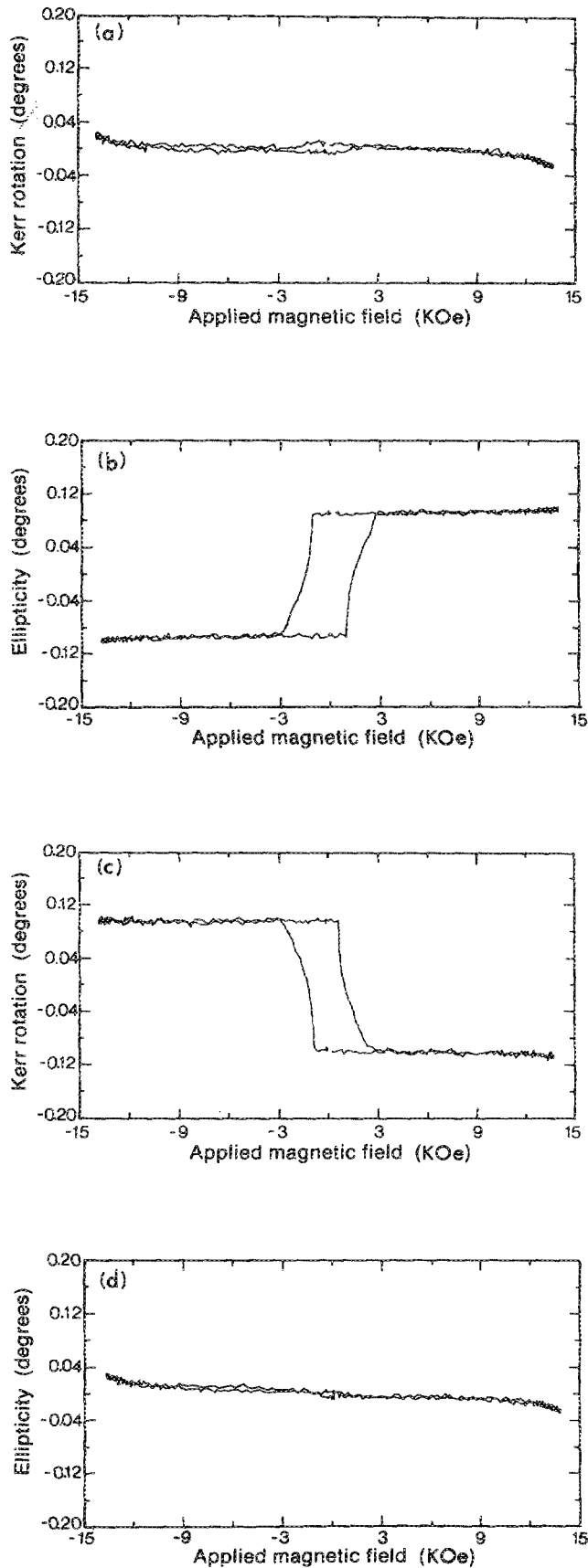


FIG. 2. (a) The polar Kerr rotation hysteresis loop and (b) the  $-1\times$  ellipticity loop of a 2-Å-Co/15.6-Å-Pd superlattice film. (c) The polar Kerr rotation hysteresis loop and (d) the  $-1\times$  ellipticity loop of the same sample after installing a quarter-wave plate.

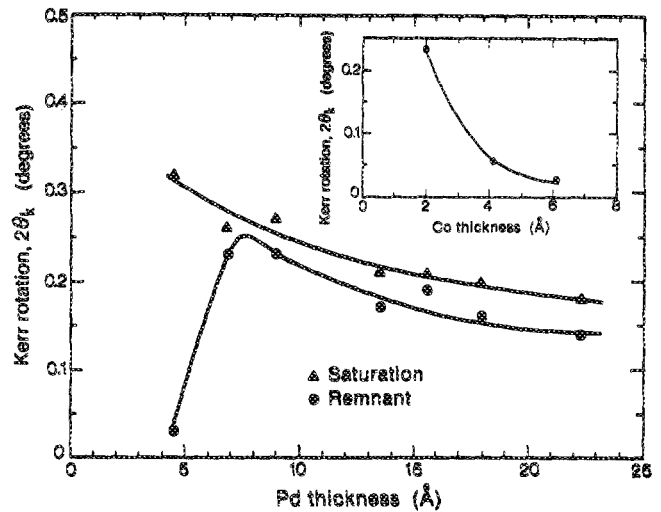


FIG. 3. The dependence of the remnant ( $H = 0$  kOe) and saturated ( $H = 15$  kOe) Kerr rotation angles on the thickness of the Pd layer. All samples had the same 2-Å-thick Co sublayer. The inset shows the dependence of the remnant Kerr rotation on the Co sublayer thickness, where all samples have the same Pd sublayer thickness of 9 Å.

was within  $\pm 5\%$ . As seen in the figure, the Kerr rotation remains constant until the thickness is down to 330 Å, and then it increases rapidly up to a maximum Kerr rotation of  $0.43^\circ$  at the film thickness of 110 Å. Optical stack calculations have shown that this enhancement can be ascribed to optical interference effects.

One of the major efforts for practical application of a magneto-optical recording medium is to enhance the carrier-to-noise ratio (CNR) for the purpose of high performance recording. Assuming that the CNR from a magneto-optical recording system is limited by shot noise in the photodetectors, the CNR is proportional to  $R\theta_K^2$ . From Fig. 4, the figure of merit of films having thicknesses between 110–270 Å is larger than any other thickness range and is therefore preferred. The maximum figure of merit occurs at a film thickness of about 200 Å in this system.

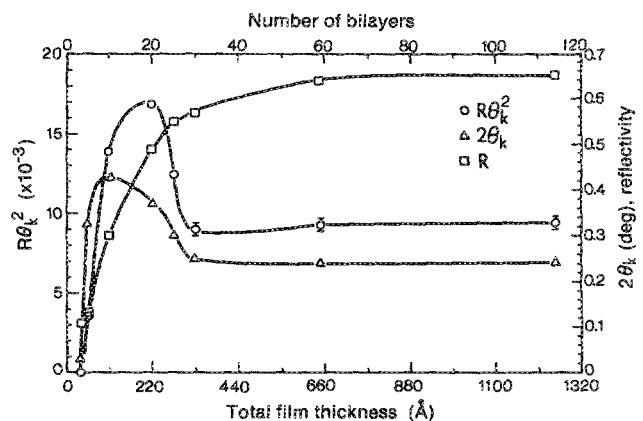


FIG. 4. The dependence of the polar Kerr rotation  $2\theta_K$ , reflectivity  $R$ , and figure of merit  $R\theta_K^2$  on the total film thickness. Each bilayer was composed of a 2-Å-thick Co and 9-Å-thick Pd.

It is worthwhile to mention that Co/Pd superlattice films have Curie temperature and coercivity suitable for application as a magneto-optical recording medium. For instance, the Curie temperature of a 2-Å-Co/9-Å-Pd superlattice film was measured to be 250 °C. Therefore, it was writable with a low-power diode laser. Furthermore, the coercivity of the sample was about 2 kOe. Thus, a micron-sized domain was found to be stable.

#### IV. CONCLUSIONS

In conclusion, we have measured the polar Kerr rotation in Co/Pd superlattice thin films. For comparison purposes, it was necessary to measure the Kerr and ellipticity hysteresis loops (at 780 nm) and calculate the maximum

Kerr rotation. In this system, the maximum polar Kerr rotation of 0.43° was observed at the total film thickness of 110 Å where each bilayer was composed of 2-Å-thick Co and 9-Å-thick Pd. The remnant polar Kerr rotation was found to be strongly dependent on both the Co/Pd sublayer thickness and the total film thickness.

<sup>1</sup>M. Kryder, *J. Appl. Phys.* **57**, 3913 (1985).

<sup>2</sup>S. C. Shin, *Appl. Phys. Lett.* **51**, 288 (1987), and references therein.

<sup>3</sup>T. K. Hatwar, S. C. Shin, and D. G. Stinson, *IEEE Trans. Magn.* **MAG-22**, 946 (1986).

<sup>4</sup>M. I. Neel, *J. Phys. Rad.* **15**, 225 (1954).

<sup>5</sup>H. J. G. Draaisma and W. J. M. de Jonge, *J. Magn. Magn. Mater.* **61**, 351 (1987).

<sup>6</sup>J. Badoz, M. Billardon, J. C. Canit, and M. F. Russel, *J. Opt.* **8**, 373 (1977).

<sup>7</sup>S. H. Jaspersen and S. E. Schnatterly, *Rev. Sci. Instrum.* **40**, 761 (1969).

<sup>8</sup>C. C. Robinson, *J. Opt. Soc. Am.* **53**, 681 (1963).